I&EC research
Industrial & Engineering Chemistry Research

Article

pubs.acs.org/IECR

Comparison of the Effectiveness of a Fluidized Sand Bath and a Steam Chamber for Reactor Heating

Heather L. Trajano,[†,‡,§] Jaclyn D. DeMartini,[†,‡,∥] Michael H. Studer,[†,‡,⊥] and Charles E. Wyman*[,†,‡]

[†]Department of Chemical and Environmental Engineering and Center for Environmental Research and Technology, Bourns College of Engineering, University of California Riverside, 1084 Columbia Avenue, Riverside, California 92507, United States

[‡]BioEnergy Science Center, Oak Ridge National Laboratory, Oak Ridge, Tennessee 37831-6422, United States

Supporting Information

ABSTRACT: Both fluidized sand baths and steam chambers have been used to heat laboratory reactors, in particular for studies of biomass pretreatment. In this study, several aspects of the heating performance of these devices were compared: time to heat reactors to reaction temperature, the stability of reactor temperature, and the convection coefficient. The convection coefficient was determined using correlations and multiple analyses of empirical data. On the basis of the results presented in this study, the steam chamber can heat reactors to temperature in a tenth of the time sand baths can, can maintain a more stable temperature during pretreatment, and has a convection coefficient one to two magnitudes greater than that of the sand bath. Therefore if heat transfer is critical, a steam chamber is advantageous.

INTRODUCTION

Heating laboratory reactors can be accomplished by a wide variety of devices. The choice of heating system is often dictated by the available equipment. A current field of research is the development of a pretreatment to alter the composition and/or structure of lignocellulosic biomass such as poplar for rapid and effective enzymatic hydrolysis as part of the efficient production of ethanol from cellulose and hemicellulose.[1] Pretreatments using water at elevated temperatures have been shown to be effective[2−11] and have been conducted in batch reactors heated in a fluidized sand bath[7,9] or more recently in a 96 well plate heated in a steam chamber[12] with improved penetration of the heat transfer fluid into the interstices between wells. This new heating device prompted an investigation into the differences in heat transfer in the traditional fluidized sand bath and the novel steam chamber in order to determine the optimal choice. Consequently, the objectives of this study were to compare (1) the time for reactors to reach reaction temperature in each device, (2) the temperature stability of the reactors during pretreatment, and (3) the convection coefficients that would describe heat transfer in each device.

CALCULATION OF CONVECTION COEFFICIENTS

The convection coefficient, h, which depends on fluid properties, surface geometry, and flow conditions[13] can be calculated with an appropriate correlation or from experimental data.

Calculation of Convection Coefficient from Literature Correlations—Sand Bath. The convection coefficient from a gas fluidized bed to a solid rod can be calculated as the sum of a gas convective component, h_g, a particle convective component, h_p, and a radiative component, h_r.[14−16]

$$h_{SB} = h_r + h_g + h_p \tag{1}$$

Since h_r is only significant at $T > 600$ °C, it was considered negligible in this study. One correlation for h_g developed by Martin is[14−16]

$$Nu_g = \frac{h_g d_p}{k_g} = 0.009 Ar^{0.5} Pr^{0.33} \tag{2}$$

The Archimedes number, Ar, and the Prandtl number, Pr, are defined in the Supporting Information.

The associated particle convective component developed by Martin is[14−16]

$$Nu_p = \frac{h_p d_p}{k_g} = (1 - \varepsilon) z (1 - e^{-N}) \tag{3}$$

where ε is the bed voidage. The characteristic group for particle convection, z, and the nondimensional contact time, N, are defined in the Supporting Information.

Molerus et al. developed an alternative prediction of the average heat transfer coefficient in a fluidized bed:[17,18]

$$Nu = \frac{h_{SB} l'}{k_g} = \frac{0.125(1 - \varepsilon_{mf})\{1 + 33.3(\sqrt[3]{\beta_1}\beta_2)^{-1}\}^{-1}}{1 + \beta_3\{1 + 0.28(1 - \varepsilon_{mf})^2 \beta_1^{-1} \beta_2^{2} \beta_4^{1.5}\}} + 0.165 Pr^{1/3} \beta_4 (1 + 0.05\beta_1^{-1})^{-1} \tag{4}$$

The parameters l', β_1, β_2, β_3, and β_4 are defined in the Supporting Information.

Received: July 18, 2012
Revised: January 15, 2013
Accepted: February 26, 2013

   dx.doi.org/10.1021/ie301869a | Ind. Eng. Chem. Res. XXXX, XXX, XXX−XXX

Finally, Zabrodsky's correlation predicts the maximum heat transfer coefficient in a fluidized bed from particle diameter and density and the thermal conductivity of the gas:[18,19]

$$h_{SB,max} = 35.7\rho_p^{0.2}k_g^{0.6}d_p^{-0.36} \quad (5)$$

Calculation of Convection Coefficient from Literature Correlations—Steam Chamber. The convection coefficient associated with the laminar film condensation of steam on the outer surface of a horizontal tube can be estimated as[13]

$$h_{SC} = 0.729\left[\frac{g\rho_l(\rho_l - \rho_v)k_l^3H_v'}{\mu_l(T_{sat} - T_{surf})d_{rod}}\right]^{1/4} \quad (6)$$

where

$$H_v' = H_v + 0.68c_{p,l}(T_{sat} - T_{surf}) \quad (7)$$

Experimental Determination of Convection Coefficients—The Energy Balance. The temperature gradient in a metal rod with radius r_0 that develops along the radius as the rod is heated from a uniform temperature T_i can be determined from an energy balance on a differential volume within the rod:[13]

$$\frac{1}{r}\frac{\partial}{\partial r}\left(k_{rod}r\frac{\partial T}{\partial r}\right) + \frac{1}{r^2}\frac{\partial}{\partial \vartheta}\left(k_{rod}\frac{\partial T}{\partial \vartheta}\right) + \frac{\partial}{\partial x}\left(k_{rod}\frac{\partial T}{\partial x}\right) + \dot{q} = \rho_{rod}c_{p,rod}\frac{\partial T}{\partial t} \quad (8)$$

For an infinite cylinder ($\partial T/\partial x = 0$) with a symmetric temperature profile ($\partial T/\partial \vartheta = 0$), constant k_{rod}, ρ_{rod}, and $c_{p,rod}$, and no energy generation within the rod ($\dot{q} = 0$), eq 8 simplifies to

$$\frac{1}{r}\frac{\partial}{\partial r}\left(k_{rod}r\frac{\partial T}{\partial r}\right) = \rho_{rod}c_{p,rod}\frac{\partial T}{\partial t} \quad (9)$$

The following initial value and boundary conditions apply for a rod in the sand bath at T_∞:

$$T(r, t = 0) = T_i \quad (10)$$

$$\left.\frac{\partial T}{\partial r}\right|_{r=0} = 0 \quad (11)$$

$$-k_{rod}\left.\frac{\partial T}{\partial r}\right|_{r=r_0} = h(T(r = r_0, t) - T_\infty) \quad (12)$$

Equations 9−12 are rewritten in terms of the following dimensionless variables in the Supporting Information:

$$\theta^* = \frac{\theta}{\theta_i} = \frac{T - T_\infty}{T_i - T_\infty} \quad (13)$$

$$t^* = Fo = \frac{\alpha_{rod}t}{r_0^2} \quad (14)$$

$$r^* = \frac{r}{r_0} \quad (15)$$

Equations 9−11 also apply to a rod in the steam chamber. However, since steam is injected into the steam chamber as the rod is heated, the temperature of the surroundings, T_∞, is a function of time; therefore, the boundary condition at $r = r_0$ must be modified to

$$-k_{rod}\left.\frac{\partial T}{\partial r}\right|_{r=r_0} = h(T(r = r_0, t) - T_\infty(t)) \quad (16)$$

Two new dimensionless temperature variables are defined:

$$\tau^* = \frac{\tau}{\tau_i} = \frac{T - T_i}{T_{\infty,ss} - T_i} \quad (17)$$

$$\tau_\infty^* = \frac{\tau_\infty}{\tau_i} = \frac{T_\infty(t) - T_i}{T_{\infty,ss} - T_i} \quad (18)$$

where $T_{\infty,ss}$ is the steady state temperature of the steam chamber. The steam chamber initial value problem is rewritten in dimensionless variables in the Supporting Information.

These initial value problems can be solved several ways as described in the following sections.

Lumped Capacitance Method. If the conduction rate is significantly larger than the convection rate, the rod's radial temperature gradient is negligible and the energy balance on the entire rod is[13]

$$-hA_s(T - T_\infty) = \rho_{rod}Vc_{p,rod}\frac{\partial T}{\partial t} \quad (19)$$

Using the dimensionless temperature, eq 13, and substituting $A = 2\pi r_0 L$ for an infinite cylinder and $V = \pi r_0^2 L$, eq 19 integrates to

$$\ln \theta^* = -\frac{2h}{\rho_{rod}r_0c_{p,rod}}t \quad (20)$$

The convection coefficient can be determined from the slope of a plot of $\ln \theta^*$ as a function of time. This method is known as the lumped capacitance model, and the error associated with neglecting the radial temperature gradient is generally small if[13]

$$Bi = \frac{hr_0}{k_{rod}} < 0.1 \quad (21)$$

Analytical Solution. The initial value problem of heating a rod in the sand bath defined by Supporting Information eqs S14−S17 can be solved precisely[13] using dimensionless variables:

$$\theta^* = \sum_{n=1}^{\infty} K_n \exp(-\zeta_n^2 Fo)J_0(\zeta_n r^*) \quad (22)$$

where

$$K_n = \frac{2}{\zeta_n}\frac{J_1(\zeta_n)}{J_0^2(\zeta_n) + J_1^2(\zeta_n)} \quad (23)$$

$$\zeta_n\frac{J_1(\zeta_n)}{J_0(\zeta_n)} = Bi = \frac{hr}{k_s} \quad (24)$$

If the Fourier number, Fo, is greater than 0.2, eq 22 can be approximated by the first term and thus the time dependence of the centerline ($r^* = 0$) temperature can be written as

$$\ln \theta^* = -\zeta_1^2\frac{\alpha}{r_0^2}t + \ln K_1 \quad (25)$$

Inspection of eqs 24 and 25 reveals that the convection coefficient can be determined from the slope of the plot of $\ln \theta^*$ as a function of time. Iteration is required in order to reach agreement between the slope and intercept of eq 25. Due to the

dx.doi.org/10.1021/ie301869a | Ind. Eng. Chem. Res. XXXX, XXX, XXX−XXX

more complex boundary conditions for the initial value problem of the steam chamber, Supporting Information eqs S18−S21 cannot be easily solved analytically.

Finite Difference Solution. The initial value problems can also be solved using finite difference methods and nonlinear fitting. By using a nonlinear least-squares solver, such as MATLAB's[20] *lsqcurvefit*, and a finite differences solver, such as MATLAB's *pdepe*, a convection coefficient that minimizes the sum of the squares of the residuals between calculated and experimental temperature profiles can be determined. The initial guess for the convection coefficient is obtained using the approaches described in previous sections.

MATERIALS AND METHODS

Thermocouple Rod. Two thermocouple rods (D = 12.7 mm, L = 150 mm) were used to determine the convection coefficients. A 3.17 mm K-type thermocouple (0.125-K-316-U-10″-T3-6 ft, Wilcon Industries, Lake Elsinore, CA) was inserted 76.2 mm into each rod along the centerline. The external portion of the thermocouple was insulated with Teflon tape. One rod was made of copper alloy 145 (9100K143, McMaster Carr, Santa Fe Springs, CA) and the other of stainless steel 316 (1305T171, McMaster Carr, Santa Fe Springs, CA). The surfaces of the rods were not modified in any way; both were smooth to the naked eye without any obvious pitting. The physical properties of the two metals are listed in Supporting Information Table S1.

Pretreatment Reactors. Custom batch reactors constructed from stainless steel piping with an outer diameter of 12.7 mm and a length of 150 mm were used for biomass pretreatment in related studies.[21] The reactors were sealed using threaded caps (SS-810-C, Swagelok, San Diego, CA). One reactor was prepared with a thermocouple (0.062-K-U-4″-T3-10 ft TF/TF-MP, Wilcon Industries, Lake Elsinore, CA) inserted along the centerline.

Heating Apparatus. The first heating apparatus was a 4-kW model SBL-2D fluidized sand bath (Techne, Princeton, NJ). The diameter of the bed was 0.23 m; at rest the height of the bed was 0.33 m. Air to fluidize the bed was provided to the base of the bed at a rate of 5.2 m^3/h at 20 °C. The density, thermal conductivity, and heat capacity of sand were assumed to be 1515 kg/m^3, 0.27 W/(m·K), and 800 J/(kg·K), respectively.[13] The surface weighted mean diameter and uniformity of the sand particles were determined to 0.134 mm and 0.262, respectively, using a Mastersizer2000 (Malvern Instruments Ltd., Malvern, U.K.).

The second heating apparatus was a custom-built steam chamber. A detailed description of this chamber was provided by Studer et al.[12] The chamber was constructed from off-the-shelf 1 MPa rated fittings. The central chamber, accessed through a ball valve, has an outer diameter of 102 mm and a length of 0.61 m and is connected to a steam boiler (FB-075-L, Fulton Companies, Pulaski, NY) and cooling water. The temperature of the chamber was measured by a K-type thermocouple located near the steam inlet to the chamber (Wilcon Industries, Lake Elsinore, CA).

Methods. During pretreatment experiments, the reactor temperature was monitored by connecting the reactor thermocouple to a Digi-Sense DualLogR Thermocouple Meter (15-176-96, Fisher Scientific, Pittsburgh, PA). Data was transferred from the meter to a computer using an infrared adapter (EW-91100-85, Cole Parmer, Vernon Hills, IL.

The thermocouple rods were heated using the same heating procedures used to heat reactors for biomass pretreatment.[21] The copper thermocouple rod was attached to the Digi-Sense DualLogR Thermocouple Meter and placed in a wire basket. The sampling interval of the Digi-Sense DualLogR Thermocouple Meter was set to one second. The sand bath was heated to 182 °C. Data collection was initiated, and then the basket and thermocouple rod were placed in the sand bath horizontally. The rod was left in the sand bath until the centerline temperature of the rod was constant for 40 to 120 s; the rod was then cooled in a 20 °C water bath. In total, three runs with each rod were performed in the sand bath, alternating between the copper and steel thermocouple rods.

The steel thermocouple rod was then inserted in the steam chamber. The boiler was preheated to an output pressure of 861 kPag, corresponding to a saturated steam temperature of 180 °C. The chamber walls were preheated by introducing steam to the chamber for approximately one minute. The flow of steam to the chamber was then stopped, and the steam in the chamber was released to atmosphere. The chamber was then flooded with cooling water for approximately one minute and then drained. After cooling, the steel thermocouple rod and steam chamber thermocouple were attached to the Digi-Sense DualLogR Thermocouple Meter, and the data sampling interval was set to one second. Data collection was initiated, and steam was introduced to the steam chamber. The temperature of the rod and steam were recorded as a function of time. Once the centerline temperature of the rod had been constant for 50 to 140 s, the flow of steam to the chamber was stopped, the steam flashed, and cooling water was introduced into the chamber.

RESULTS AND DISCUSSION

Reactor Heating Time. An important measure of the heating performance of the sand bath and steam chamber is the time for a bundle of 10 mL stainless steel pretreatment reactors to reach the desired reaction temperature, which in a recent study was 180 °C.[21] The average time to reach 178 °C in the sand bath was 3.10 ± 0.35 min while the average heat-up time in the steam chamber was 0.39 ± 0.10 min. This reduced heating time reflects the better heat transfer properties of steam relative to fluidized sand while the reduced standard deviation of the heating time in the steam chamber is a reflection of the immutable physical properties of steam.

Stability and Consistency of Reactor Temperature. Another important aspect of heating during pretreatment is the stability of the temperature during the reaction. Representative sample temperature profiles from a pretreatment in the sand bath and in the steam chamber are shown in Figure 1.[21] This figure demonstrates that there was less variation in the temperature of the reactors during a run when the steam chamber was used reflecting the temperature stability of the surroundings. The fluctuations in the sand bath temperature are due to the on/off response of the TC-8D temperature controller (Techne, Princeton, NJ), while the boiler pressure and thus steam chamber temperature was more stable because of a subtler controller response. In addition, it is likely that conditions within the sand bath are not completely homogeneous, thus increasing temperature fluctuations.

Sand Bath Convection Coefficient—Calculated by Correlation. The sand bath convection coefficient was predicted with the correlations developed by Martin, Molerus et al., and Zabrodsky.[14,15,17,19] The physical properties of air were evaluated at atmospheric pressure at 182 °C. The bed

dx.doi.org/10.1021/ie301869a | Ind. Eng. Chem. Res. XXXX, XXX, XXX−XXX

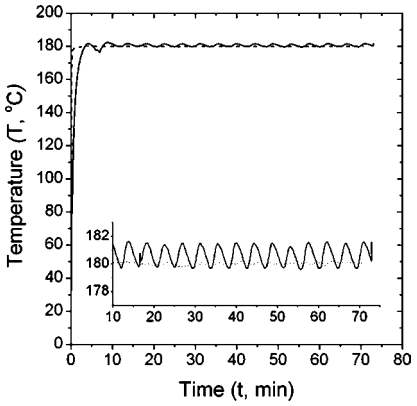

Figure 1. Temperature profiles of nine tube reactors during pretreatment at 180 °C for 69.9 min in the fluidized sand bath (solid line) and steam chamber (dotted line). The inset is a magnification of the same data from 10 to 75 s.

voidage at minimum fluidization and operating conditions was estimated to be 0.38 and 0.59, respectively, from force balances on the bed.[14,21] Sensitivity analyses in which relevant variables were changed by ±25% were conducted for each correlation.

The convection coefficient of the sand bath at 182 °C was calculated to be 453 W/(m^2·K) using the Martin correlation, eqs 1−3.[14,15] The sensitivity analysis showed that changes in the particle size, bed voidage at minimum fluidization, sand density, accommodation coefficient, sand heat capacity, or conductivity changed the prediction of the convection coefficient by less than 15%. Increasing the experimental Martin[14,15] constant to 4 resulted in a convection coefficient of just 295 W/(m^2·K), but as C was validated for a wide range of operating conditions[15] it is unlikely that Martin's recommended value of 2.6 is invalid. Twenty-five percent variation in bed voidage resulted in 28% decrease in the predicted convection coefficient; therefore, a second sensitivity analysis of the variables influencing the calculation of bed voidage was conducted. A ±25% variation in sand and air density, particle size, air viscosity, and superficial velocity resulted in 0.10−13% changes in the bed voidage indicating that a 25% adjustment in bed voidage is unlikely and thus a large variation in the convection coefficient is also unlikely.

The convection coefficient of the fluidized sand bath at 182 °C was estimated to be 228 W/(m^2·K) based on the Molerus correlation.[17] The ±25% sensitivity analysis showed that changes in sand properties, bed voidage, and bed voidage at minimum fluidization alter the prediction of the sand bath convection coefficient by 0.6−11%. The Molerus prediction of the convection coefficient is approximately half that predicted using Martin's equations.[14,15] However, as will be shown below, the Martin correlation[14,15] more closely matches the convection coefficients predicted empirically; therefore, in this study, it appears that the Martin correlation[14,15] is the better choice.

The maximum convection coefficient of the fluidized sand bath at 182 °C was determined to be 535 W/(m^2·K) with the Zabrodsky correlation,[19] which is comparable to the prediction by the Martin[14,15] correlation. The ±25% sensitivity analysis demonstrated that inaccuracies in the particle size, particle density, or gas conductivity change the estimate of the maximum possible convection coefficient by less than 16%.

Sand Bath Convection Coefficient—Calculated by Lumped Capacitance. By fitting a linear regression model to a plot of the natural logarithm of the nondimensional temperature as a function of time multiplied by $-2/(\rho_{rod} r_0 c_{p,rod})$, the first calculation of the convection coefficient from sand bath experimental data was completed using the lumped capacitance method, eq 20. A sample plot using data from the copper thermocouple rod is shown in Figure 2. The

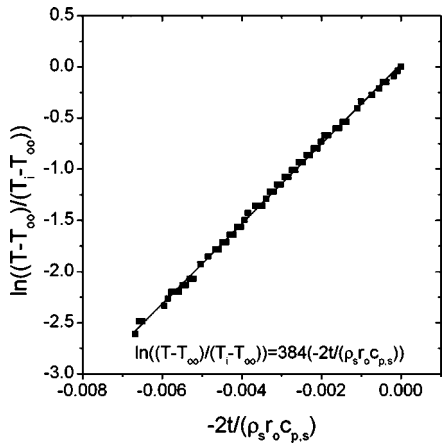

Figure 2. Dimensionless centerline temperature of the copper thermocouple rod (run 2) in the sand bath as a function of modified time. By the assumption of lumped capacitance, the slope of the line is equal to the convection coefficient (eq 20).

average convection coefficients and associated standard deviation from three runs with the copper and steel thermocouple rods were 381 ± 18 W/(m^2·K) and 365 ± 4 W/(m^2·K), respectively. Because the associated Biot numbers were 0.0063 and 0.17, respectively, the lumped capacitance assumption was valid only for the copper thermocouple rod.

Sand Bath Convection Coefficient—Calculated by Analytical Solution. The lumped capacitance assumption proved invalid for the steel thermocouple rod; therefore, the rod's radial temperature gradient was accounted for by using eq 25 as shown in Figure 3. Since the slope and intercept of this model are both dependent on ζ_1, as defined by eqs 23 and 24, iteration was required to reach agreement between eqs 23, 24, and 25. By this analysis, the average convection coefficient and associated standard deviation from three runs with the copper and steel thermocouple rods were 374 ± 23 W/(m^2·K) and 392 ± 4.7 W/(m^2·K), respectively. As with the lumped capacitance approach, the results from the copper and steel thermocouple rod are in close agreement.

Sand Bath Convection Coefficient—Calculated by Finite Differences Solution. The initial value problem posed by eqs 9−12 was also solved numerically. The solutions obtained in the previous sections were used as initial guesses for the convection coefficient; initial guesses bracketing these values were also used. The equations were solved using three different increment sizes in the radial direction: 0.1, 0.01, and 0.001.

Table 1 summarizes the convection coefficients for run 1 with the copper thermocouple rod for each initial guess using each radial mesh. Thus, it can be seen that the calculated convection coefficient only changed by 0.66% as radial mesh size was decreased from 0.1 to 0.001, demonstrating there is little benefit in further decreasing the radial mesh. The convection coefficient for the remaining runs was calculated using a mesh size of 0.001. It can also be seen from Table 1 that

dx.doi.org/10.1021/ie301869a | Ind. Eng. Chem. Res. XXXX, XXX, XXX−XXX

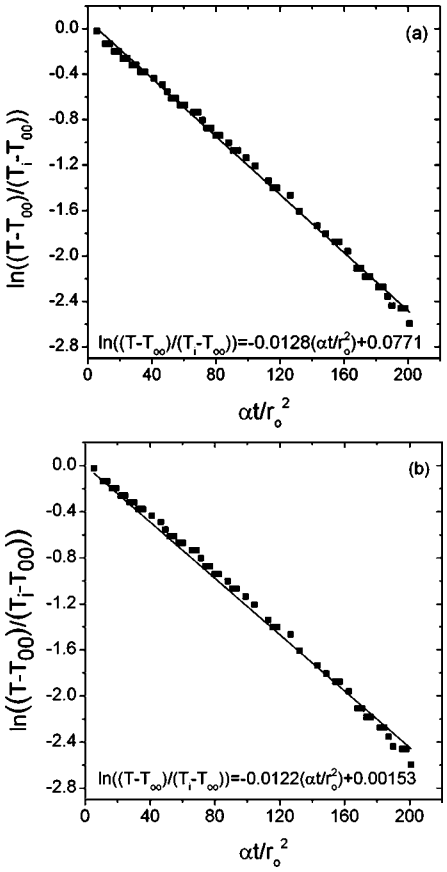

Figure 3. Dimensionless centerline temperature of the copper thermocouple rod (run 2) in the sand bath as a function of dimensionless time. Initial linear fit of eq 25 to the data (a). Linear fit of eq 25 to the data after iteration to reach agreement between eqs 23 and 24 (b).

the initial guess does not influence the final convection coefficient; thus, the convection coefficient for subsequent runs was calculated using the solutions from the previous sections.

The average convection coefficients from three runs using the copper and steel thermocouple rods were determined, using a finite elements analysis with a radial mesh of 0.001, to be 366 ± 8.6 W/(m²·K) and 375 ± 6.7 W/(m²·K), respectively. There was a mere 2.3% difference in these values.

Comparison of Calculated Sand Bath Convection Coefficients. With the exception of the Molerus correlation,[17] the calculated sand bath convection coefficients cover a relatively narrow range of 365 W/(m²·K) to 481 W/(m²·K), providing confidence that the true convection coefficient of the sand bath is within this range. It is interesting to note that the Martin and Zabrodsky correlations predict convection coefficients up to 31% greater than the convection coefficients calculated from experimental data. This could reflect the influence of the steel basket used to lower the thermocouple rod into the sand bath. The steel thermocouple rod was used in order to reproduce reactors used for biomass pretreatment while the copper thermocouple rod was used to minimize the radial temperature gradient. The convection coefficients calculated using data from the copper thermocouple rod agree with the convection coefficients calculated using the steel thermocouple rod. This is as expected since the convection coefficient represents the heat transfer from the sand bath and should only be influenced by rod geometry and bed conditions.

Steam Chamber Convection Coefficient—Calculated by Correlation. The convection coefficient for the steam chamber was estimated as a function of time using eq 6, with the results plotted in Figure 4. The properties of the vapor and the enthalpy of vaporization were evaluated at the steam temperature, and the properties of the saturated liquid were evaluated at the film temperature. The film temperature was assumed to be the average of the steam and centerline temperature. The convection coefficients estimated in this manner ranged from approximately 10428 W/(m²·K) to 26576 W/(m²·K), an extremely large variation. The correlation predicted an increase in the convection coefficient with increasing time due to the increase in the enthalpy of vaporization with increasing steam temperature and a decrease in the difference between the steam chamber and thermocouple rod temperature.

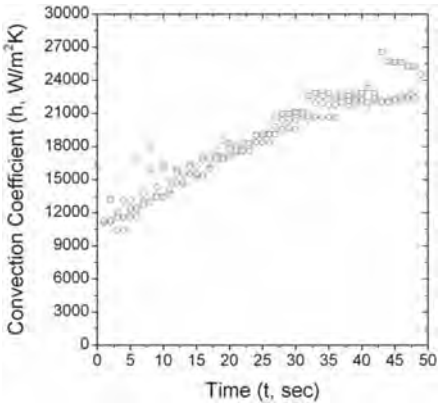

Figure 4. Convection coefficient of steam chamber predicted with eq 6 as a function of time. □, run 1; ◇, run 2; ○, run 3.

Steam Chamber Convection Coefficient—Calculated by Lumped Capacitance. The first attempt to estimate the convection coefficient was based on the assumption of lumped

Table 1. Convection Coefficients from the Finite Differences Approximation Solution for Copper Rod Run 1

source of initial guess	initial guess, h_0 (W/(m²·K))	h for $\Delta r = 0.1$ (W/(m²·K))	h for $\Delta r = 0.01$ (W/(m²·K))	h for $\Delta r = 0.001$ (W/(m²·K))	h_{avg} (W/(m²·K))
	1	369	368	367	368 ± 1.1
Molerus correlation[17]	198	369	368	367	368 ± 1.1
lumped capacitance	389	369	368	367	368 ± 1.1
analytical solution	398	369	368	367	368 ± 1.1
Martin correlation[14,15]	436	369	368	367	368 ± 1.1
Zabrodsky correlation[19]	481	369	368	367	368 ± 1.1
	1000	369	368	367	368 ± 1.1

dx.doi.org/10.1021/ie301869a | Ind. Eng. Chem. Res. XXXX, XXX, XXX−XXX

capacitance. Since the steam chamber temperature was not constant, the lumped capacitance method cannot be accurately applied, but the result does provide an initial guess to the finite differences solution. The steady state steam chamber temperature, 180 °C, was used to calculate a convection coefficient of 1508 ± 288 W/(m^2·K), with the corresponding Biot number of the rod determined to be 0.71. This large Biot number indicated there was a radial temperature gradient within the thermocouple rod and that the lumped capacitance approach is invalid.

Steam Chamber Convection Coefficient—Calculated by Analytical Solution. A second initial guess for the finite differences solution was determined by applying the analytical solution, eqs 23−25, assuming a constant steam chamber temperature of 180 °C. The average convection coefficient was found to be 2097 ± 583 W/(m^2·K).

Steam Chamber Convection Coefficient—Calculated by Finite Differences Solution. In order to determine the steam chamber convection coefficient by the finite differences approach, an equation describing the steam chamber temperature as a function of time was needed. This equation must have the properties described by Supporting Information eqs S22−S24; accordingly, the following function was used:

$$T = f(t) = a + b\,\exp(-t/c) \tag{26}$$

Parameters a, b, and c were determined for each run using the dimensionless variables defined by eqs 14 and 17. No solution that minimized the sum of the squares of the residuals was found as this value was shown to be an asymptotic function of the convection coefficient. To address this, the previous approach was modified to determine a convection coefficient that would match the predicted time to reach 178 °C, $t_{pred,178}$, to the experimental time, $t_{exp,178}$, using MATLAB's *fzero* function. Run 1 is used as a representative example; two possible roots, 365 and 1080 W/(m^2·K), were calculated, and the experimental and predicted temperature profiles for each root are plotted in Figure 5. Neither root adequately describes the system, with the result that the finite differences method provided no usable values of the steam chamber convection coefficient.

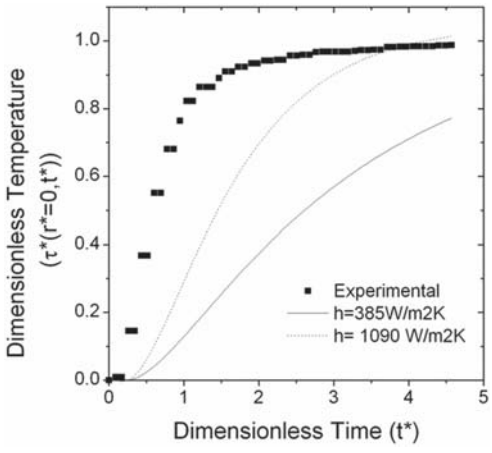

Figure 5. Comparison of dimensionless experimental centerline temperature of the steel thermocouple rod in the steam chamber to those predicted for convection coefficients of 385 W/(m^2·K) (solid line) and 1090 W/(m^2·K) (dotted line) as a function of dimensionless time.

Comparison of Calculated Steam Chamber Convection Coefficients. The calculated steam chamber convection coefficients ranged from 1508 W/(m^2·K) to 26576 W/(m^2·K). The results could be improved if the design of the steam chamber could be modified so that the chamber could reach a steady state temperature prior to the heating of the steel thermocouple rod. This would create a steady state boundary condition and reduce the solution of Supporting Information eqs S18−S19 to that of Supporting Information eqs S14−S17. However, implementation of such a system would be very challenging.

Comparison of Convection Coefficients of Sand Bath and Steam Chamber. Both the sand bath and steam chamber use a fluid to transfer heat from resistance heaters to thermocouple rods or reactors; the convection coefficient of each system reflects the efficiency of this transfer. Calculated convection coefficients of the steam chamber were at least 1 order of magnitude larger than the calculated sand bath convection coefficients. Inspection of eqs 1−3 and Supporting Information S1−S3 reveals that the sand bath convection coefficient increases with the heat capacity of sand and air, as well as the thermal conductivity of air, while inspection of eqs 6 and 7 shows that the steam chamber convection coefficient increases with the heat capacity and thermal conductivity of saturated liquid water, as well as the enthalpy of vaporization. From Supporting Information Table S5 it is clear that the thermal conductivity and heat capacity of saturated liquid water in the steam chamber is substantially higher than that of air and sand in the fluidized sand bath. And, of course, the enthalpy of vaporization of water is very high at 2257 kJ/kg. Thus the high thermal conductivity, heat capacity, and enthalpy of vaporization of steam all contribute to the high steam chamber convection coefficient.

■ CONCLUSIONS

The heat transfer by two heating systems, a fluidized sand bath and a steam chamber, were compared as part of the Wyman lab's biomass pretreatment research. There were significant differences in the heating performances of the two systems. The steam chamber heated pretreatment tube reactors to 178 °C in approximately a tenth of the time it took the sand bath to do so, reflecting the improved heat transfer from the heat transfer medium to the reactors. The temperature of the pretreatment reactors in the steam chamber was also more stable than the temperature of the pretreatment reactors in the sand bath, likely due to better temperature control and more constant medium temperature.

The convection coefficient of each device was determined from data collected using custom-designed thermocouple rods. Analysis of the data by multiple approaches indicated that the convection coefficient of the steam chamber was 1 to 2 orders of magnitude greater than that of the sand bath.

Overall, because the heat transfer performance of the steam chamber was superior to that of the sand bath in all aspects, a steam chamber should be utilized for critical heat transfer experiments.

■ ASSOCIATED CONTENT

Supporting Information

Variables associated with the Martin and Molerus correlations, statements of initial value problems associated with the heating of the sand bath and steam chamber in dimensionless variables, and requirements of the function describing the steam chamber

dx.doi.org/10.1021/ie301869a | Ind. Eng. Chem. Res. XXXX, XXX, XXX−XXX

temperature as a function of time. Tables summarizing the physical properties of copper and stainless steel (the thermocouple rod materials) as well as sand, air, and saturated liquid water at 180 °C are also supplied. This information is available free of charge via the Internet at http://pubs.acs.org/.

AUTHOR INFORMATION

Corresponding Author

*Tel: 951-781-5703. Fax: 951-781-5790. E-mail: charles.wyman@ucr.edu.

Present Addresses

[§]H.L.T.: Chemical and Biological Engineering, University of British Columbia, 3620 East Mall, Vancouver, BC, Canada V6T 1Z3.

[∥]J.D.D.: Genencor, 925 Page Mill Road, Palo Alto, CA 94304, USA.

[⊥]M.H.S.: Institute of Process Engineering, Swiss Federal Institute of Technology (ETH Zurich), Sonneggstr. 3, CH-8092 Zurich, Switzerland.

Notes

The authors declare the following competing financial interest(s): C.E.W. is cofounder of Mascoma Corporation and chair of their Scientific Advisory Board. C.E.W. is also member of the Scientific Advisory Board of Mendel Biotechnology, Inc.

ACKNOWLEDGMENTS

This research was made possible through support of the BioEnergy Science Center (BESC), a U.S. Department of Energy Bioenergy Research Center supported by the Office of Biological and Environmental Research in the DOE Office of Science. The corresponding author is also grateful to the Ford Motor Company for funding the Chair in Environmental Engineering at the Center for Environmental Research and Technology of the Bourns College of Engineering at UCR that augments support for many projects such as this.

REFERENCES

(1) Mosier, N.; Wyman, C.; Dale, B.; Elander, R.; Lee, Y. Y.; Holtzapple, M.; Ladisch, M. Features of Promising Technologies for Pretreatment of Lignocellulosic Biomass. *Bioresour. Technol.* **2005**, *96*, 673.

(2) Allen, S. G.; Schulman, D.; Lichwa, J.; Antal, M. J., Jr.; Jennings, E.; Elander, R. A Comparison of Aqueous and Dilute Acid Single Temperature Pretreatment of Yellow Poplar Sawdust. *Ind. Eng. Chem. Res.* **2001**, *40*, 2352.

(3) Heitz, M.; Capek-Menard, E.; Koerberle, P. G.; Gagne, J.; Chornet, E.; Overend, R. P.; Taylor, J. D.; Yu, E. Fractionation of *Populus tremuloides* at the Pilot Plant Scale: Optimization of Steam Pretreatment Conditions Using the STAKE II Technology. *Bioresour. Technol.* **1991**, *35*, 23.

(4) Negro, M. J.; Manzanares, S. P.; Ballesteros, I.; Oliva, J. M.; Cabanas, A.; Ballesteros, M. Hydrothermal Pretreatment Conditions to Enhance Ethanol Production from Poplar Biomass. *Appl. Biochem. Biotechnol.* **2003**, *105*, 87.

(5) Tucker, M. P.; Farmer, J. D.; Keller, F. A.; School, D. J.; Nguyen, Q. A. Comparison of Yellow Poplar Pretreatment Between NREL Digester and Sunds Hydrolyzer. *Appl. Biochem. Biotechnol.* **1998**, *70–72*, 25.

(6) Bobleter, O. Hydrothermal Degradation of Polymers Derived from Plants. *Prog. Polym. Sci.* **1994**, *19*, 797.

(7) Kim, Y.; Mosier, N. S.; Ladisch, M. R. Enzymatic Digestion of Liquid Hot Water Pretreated Hybrid Poplar. *Biotechnol. Prog.* **2009**, *25*, 340.

(8) Bonn, G.; Concin, R.; Bobleter, O. Hydrothermolysis- A New Process for the Utilization of Biomass. *Wood Sci. Technol.* **1983**, *17*, 195.

(9) Lloyd, T.; Wyman, C. E. Combined Sugar Yields for Dilute Sulfuric Acid Pretreatment of Corn Stover Followed by Enzymatic Hydrolysis of the Remaining Solids. *Bioresour. Technol.* **2005**, *96*, 1967.

(10) Grous, W. R.; Converse, A. O.; Grethlein, H. E. Effect of Steam Explosion Pretreatment on Pore Size and Enzymatic Hydrolysis of Poplar. *Enzyme Microb. Technol.* **1986**, *8*, 274.

(11) Brownell, H. H.; Saddler, J. N. Steam Pretreatment of Lignocellulosic Material for Enhanced Enzymatic Hydrolysis. *Biotechnol. Bioeng.* **1987**, *25*, 228.

(12) Studer, M. H.; DeMartini, J. D.; Brethauer, S.; McKenzie, H. L.; Wyman, C. E. Engineering of a High-Throughput Screening System to Identify Cellulosic Biomass, Pretreatments, and Enzyme Formulations That Enhance Sugar Release. *Biotechnol. Bioeng.* **2010**, *105*, 231.

(13) Incropera, F. P.; DeWitt, D. P. *Introduction to Heat Transfer*; John Wiley and Sons: New York, 2002.

(14) Martin, H. Heat Transfer Between Gas Fluidized Beds of Solid Particles and the Surfaces of Immersed Heat Exchanger Elements, Part I. *Chem. Eng. Proces.* **1984**, *18*, 157.

(15) Martin, H. Heat Transfer Between Gas Fluidized Beds of Solid Particles and the Surfaces of Immersed Heat Exchanger Elements, Part II. *Chem. Eng. Proces.* **1984**, *18*, 199.

(16) Ackeskog, H. B. R.; Almstedt, A. E.; Zakkay, V. An Investigation of Fluidized Bed Scaling: Heat Transfer Measurements in a Pressurized Fluidized-Bed Combustor and a Cold Model Bed. *Chem. Eng. Sci.* **1993**, *48*, 1459.

(17) Molerus, O.; Burschka, A.; Dietz, S. Particle Migration at Solid Surfaces and Heat Transfer in Bubbling Fluidized Beds- II. Prediction of Heat Transfer in Bubbling Fluidized Beds. *Chem. Eng. Sci.* **1995**, *50*, 879.

(18) Pisters, K.; Prakash, A. Investigations of Axial and Radial Variations of Heat Transfer Coefficient in Bubbling Fluidized Bed with Fast Response Probe. *Powder Technol.* **2011**, *207*, 224.

(19) Zabrodsky, S. S. *Hydrodynamics and Heat Transfer in Fluidized Beds*; M.I.T. Press: Cambridge, 1966.

(20) MathWorks Inc. *MATLAB 2011b* [computer program]; Natick, MA, 2011.

(21) McKenzie, H. L. Tracking Hemicellulose and Lignin Deconstruction During Hydrothermal Pretreatment of Biomass. Ph.D. Thesis, University of California Riverside, Riverside, CA, June 2012.